ISBN: 978-3-95450-184-7 doi:10.18429/JACoW-IPAC2018-TUPMF027

IMPEDANCE MODELING FOR eRHIC*

A. Blednykh†, G. Bassi, M. Blaskiewicz, C. Hetzel, V. Ptitsyn, V. Smalyuk, F. Willeke
Brookhaven National Laboratory, Upton, NY 11973, USA

Abstract

The impedance budget for the eRHIC project is discussed at its earlier stage of development. As a first step, with the eRHIC lattice and beam parameters, we use the geometric impedances of the vacuum chamber components simulated for the NSLS-II project. The impedance budged will be updated next with more impedance data simulated for the optimized eRHIC vacuum components. It will allows us to keep track on the collective effects changes with more realistic components added to the ring.

INTRODUCTION

A new electron ion collider (eRHIC) is under design at BNL. The 10GeV electron ring with a 3833.845m circumference is taken for consideration with a 60° FODO lattice [1]. The main parameters of the electron ring lattice to study collective effects are given in Table 1. For the estimation of the instability thresholds, the most accurate approach is to perform particle tracking simulations with the wakefields obtained numerically for the vacuum components distributed around the ring.

Table 1: Parameter for Threshold Calculations

Energy	E[GeV]	10
Revolution Period	T_0[μs]	12.79
Momentum Compaction	α	1.45 $\times 10^{-3}$
Energy Loss	U[keV]	9100
RF Voltage	V[MV]	41
Synchrotron tune	ν_s	0.0815
Damping Time	τ_x, τ_s[ms]	70, 35
Energy Spread	σ_δ	5.65 $\times 10^{-4}$
Bunch Length	σ_s[mm]	20

LONGITUDINAL IMPEDANCE MODEL

The electron beam, by passing through the vacuum chamber, generates electromagnetic fields, which can affect the beam stability at much lower beam intensity than the designed parameters. Hence, it is important to determine the impedance/wakepotential of all vacuum components distributed around the ring, which are seen by the electron beam. The preliminary vacuum components list is presented in Table 2 at its earlier stage. The geometric dimensions and the surface resistivity of many vacuum components are not known yet. As a first attempt to estimate the instability thresholds, we apply the wakepotential/impedance simulated for the NSLS-II vacuum components [2] with the eRHIC main lattice parameters. The geometric impedance due to cross-section changes in the vacuum components has been calculated by the GdfidL code [3]. Based on the status of the simulations, the vacuum components are marked as the NSLS-II project or the eRHIC project, based on the applied wakepotential. With more updates in the geometries and their optimization from an impedance point of view for the eRHIC project, the NSLS-II wakepotential/impedance will be replaced individually and those new wakepotentials/impedances will be used to generate the total impedance budget for particle tracking simulations and for theoretical analysis. Concerning the resistive wall impedance, its contribution to the total impedance is calculated separately by applying the analytical approach derived by Bane and Sands [4].

$$W_{||}(s) = \frac{r_e mc^2 N_e}{2b\sqrt{2\mu_r Z_0 \sigma_{con}}} \left|\frac{s}{\sigma_s}\right|^{3/2} e^{-s^2/4\sigma_s^2} \times \left[I_{1/4}\left(\frac{s^2}{4\sigma_s^2}\right) - I_{-3/4}\left(\frac{s^2}{4\sigma_s^2}\right) + sgn(s) I_{-1/4}\left(\frac{s^2}{4\sigma_s^2}\right) - sgn(s) I_{3/4}\left(\frac{s^2}{4\sigma_s^2}\right)\right], \quad (1)$$

where b is the vacuum chamber radius, $Z_0 = 120\pi$ is the impedance of free space, σ_{con} is the electrical conductivity, μ_r is the relative permeability of the chamber surface, N_e is the electron bunch population and I_α are the modified Bessel functions of first kind. As a preliminary estimation, for the resistive wall surface, 6 arc sections with 257m of Cu and with radius of b = 20mm and 12 straight sections made each of 123m in length (Cu) with radius of b = 20mm are taken into account.

Table 2: List of the vacuum components contributing to the total preliminary impedance of the electron ring.

Object	Symbol	Number of components	Wakefield
Bellows	BLW	380	NSLS-II
LA BPM	LABPM	494	NSLS-II
Stripline	SL	18	NSLS-II
Gate Valve	GV	45	NSLS-II
Flange Absorber	FABS	200	NSLS-II
RF Cavity	CAV	23	NSLS-II
RF Tapered Transition	TPRDRF	—	—
IR Chamber	IRCHM	—	—

To estimate the instability thresholds for the electron ring, an approximation to the wakepotential for a 0.3mm bunch length is used for beam dynamics simulations, a bunch length

* Work supported by Brookhaven Science Associates, LLC under Contract No. DE-AC02-98CH10886 with the U.S. Department of Energy
† blednykh@bnl.gov

ISBN: 978-3-95450-184-7 doi:10.18429/JACoW-IPAC2018-TUPMF027

much shorter than the 20mm length of the unperturbed circulating bunch. The total longitudinal wakepotential (blue trace) as a sum of the short-range geometric (orange trace) and resistive-wall (green trace) longitudinal wakepotentials is shown in Fig. 1. The frequency spectrum of the real part of the total longitudinal impedance is presented in Fig. 2 up to 350GHz (green trace).

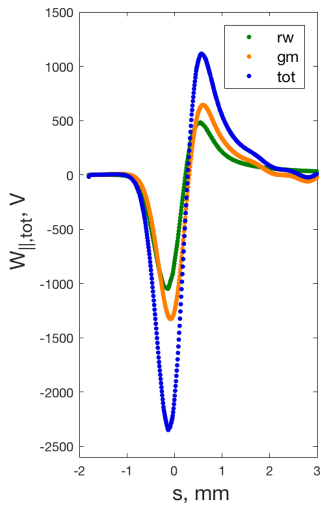

Figure 1: The longitudinal short-range wakepotential calculated for a $\sigma_s = 0.3$mm bunch length (WMar62018). The total longitudinal wakepotential of the eRHIC project (blue trace) is a sum of the resistive wall contribution (green trace), calculated analytically with Eq. 1, and the geometric wakepotentials (orange trace).

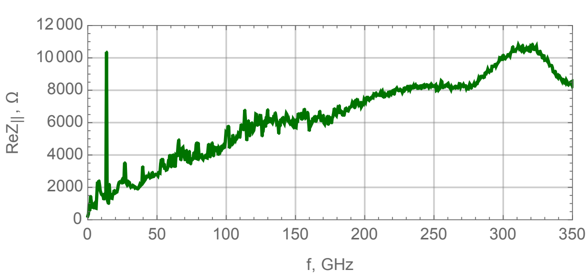

Figure 2: Real part of the longitudinal impedance

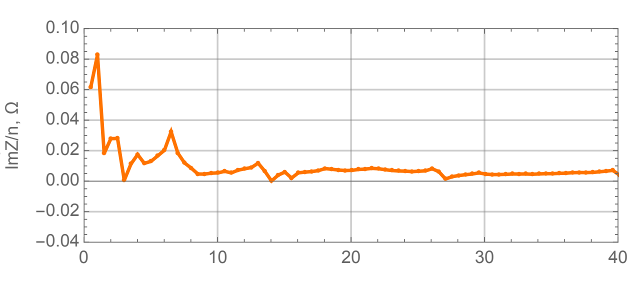

Figure 3: imaginary part of the longitudinal impedance divided by $n = \omega/\omega_0$, where $\omega_0 = 2\pi \times 78.186$kHz

The computed total longitudinal wakepotential $W_{||,tot}$ is used as input file for the SPACE particle tracking code [5] for beam dynamics simulations, with parameters is given in Table 1. The numerical simulations are done using 30M macro particles and 800 grid points, in order to accurately determine the first microwave instability threshold and to characterize the microwave dynamics above it. The energy spread of the unperturbed Gaussian bunch at low current is $\sigma_\delta = 5.65 \times 10^{-4}$. The first microwave instability threshold is observed at $I_{th} = 4.5$mA (Fig. 4), which is above the single bunch current 3.8mA. For the applied total longitudinal wakepotential, the increase in bunch length due to potential well-distortion (Fig. 5) is small, approximately 10% at the first microwave instability threshold.

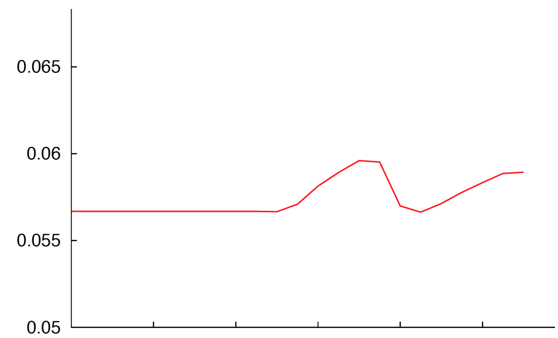

Figure 4: Energy spread as a function of single bunch current

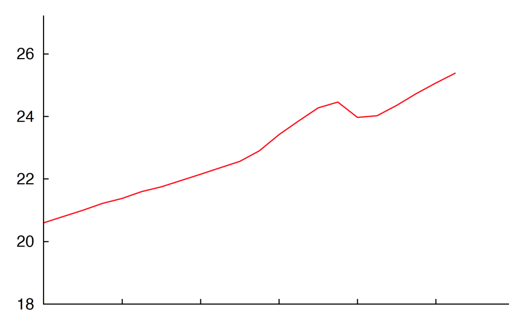

Figure 5: Bunch lengthening dependence on single bunch current.

BETATRON TUNE DEPENDENCE ON ELECTRON BEAM INTENSITY

For the octagonal shape of the dipole vacuum chamber with a half-aperture $b = 20$mm and dipole magnet half-gap $d = 26$mm, the multi-bunch current dependent betatron tune shift induced by the quadrupole impedance of the dipole magnets at frequency $\omega \to 0$ is given by

$$\Delta\nu_{x,y} = \frac{I_{av} L}{4\pi E/e} \beta_{x,y} Im Z_{Q_{x,y}}(0), \quad (2)$$

where $L = 192 \times 6.064$m is the total length of the dipole magnets, $I_{av} = 2.48$A is the average current, $\beta_x = 17$m and $\beta_y = 18$m are the local horizontal and vertical average

ISBN: 978-3-95450-184-7 doi:10.18429/JACoW-IPAC2018-TUPMF027

beta functions, $E = 10$GeV is the electron beam energy and $ImZ_{Q_{x,y}}$ is the imaginary part of the quadrupole impedance. For the dipole magnets, the quadrupole impedance $ImZ_{Q_{x,y}}$ is analytically approximated by a multi-parallel plates model [6]

$$ImZ_{Q_{x,y}}(0) = \pm\frac{\pi^2}{12cb^2}\left(1 + 2\frac{b^2}{d^2}f(\eta)\right), \tag{3}$$

where

$$f(\eta) = \frac{6}{\pi^2}Li_2(\eta), \tag{4}$$

and

$$\eta = \frac{\mu_r - 1}{\mu_r + 1}. \tag{5}$$

With relative permeability $\mu_r \to 0$ (perfect magnets) $f(\eta) = 1$. We notice that Eq. (3) differs by a factor of 2 from the formula for the resistive wall impedance derived by Chao, Heifets and Zotter in Ref. [7] using the well known Laslett coefficients [8]. The validity of Eq.(2), where the only contribution to the betatron tune shift is given by the quadrupole impedance evaluated at zero frequency, is justified by the fact that the first contribution from the dipole impedance, which is given by the impedance evaluated at $\nu_\perp f_0$, where $\nu_\perp$ is the fractional betatron tune and $\perp = x$ or y, is negligible, as shown in Fig.6 for the nominal fractional betatron tunes $\nu_x = 0.08$ and $\nu_y = 0.06$.

The calculated betatron tunes ν_x and ν_y as a function of average current I_{av} are presented in Fig. 7. At the nominal $I_{av} = 2.48$A, the estimated tune shifts $\Delta\nu_x = 0.05$ and $\Delta\nu_y = -.05$ might affect the lattice optimization to mitigate the beam-beam interaction [1]. To eliminate the effect of the quadrupole impedance on the multi-bunch tune shift dependence vs the average current, the dipole vacuum chamber should be considered with a circular profile.

CONCLUSION

Work on the eRHIC impedance budget is in progress. The instability thresholds will be re-calculated based upon the wakefields of the real eRHIC vacuum components. The vacuum chamber with a circular profile will be predominantly considered for the multipole and dipole magnets with the purpose to eliminate the betatron tune shift dependence vs. average current caused by the quadrupole impedance at low frequencies.

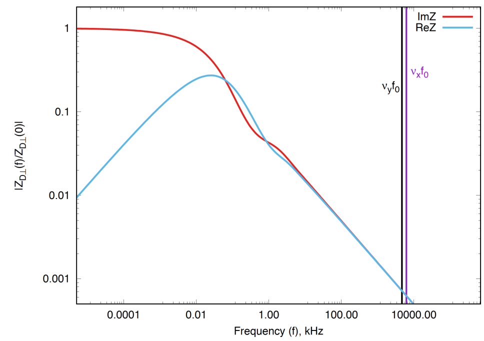

Figure 6: Absolute value of the ratio of the transverse dipole impedance to the quadrupole impedance evaluated at zero frequency. Here $\perp$ is either x or y. The dipole and quadrupole impedances are related as follows: $Z_{D_x}(f) = -Z_{Q_x}(f)$, $Z_{D_y}(f) = Z_{Q_y}(f)$. The dipole impedance is obtained numerically by the standard field matching technique as applied in [6], with dipole chamber conductivity $\sigma_{Cu} = 54S/$m and thickness $t = 3$mm. The dipole impedance, evaluated at $f = \nu_\perp f_0$ with parameters $\nu_x = 0.08$, $\nu_y = 0.06$ and $f_0 = 78196.5$kHz, is negligible with respect to the quadrupole impedance evaluated at $f = 0$, thus justifying the validity of Eq.(2).

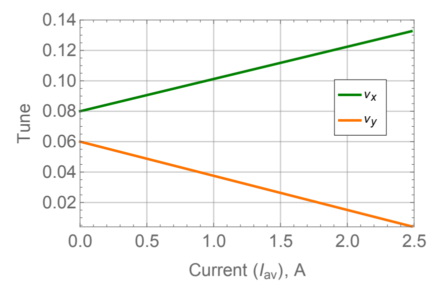

Figure 7: Horizontal and vertical betatron tune shifts as a function of average current estimated using Eq.(2).

REFERENCES

[1] The eRHIC Pre-Conceptual Design Report 2018.

[2] A. Blednykh, Impedance modeling in low emittance ring, ICFA Mini-Workshop on Impedances and Beam Instabilities in Particle Accelerators, Benevento, September 19-22, 2017.

[3] W. Bruns, www.gdfidl.de.

[4] K. Bane and M. Sands, Short-Range Resistive Wall Wakefields, AIP Conf. Proc. 367, 131 (1996).

[5] G. Bassi, A. Blednykh and V. Smaluk, Phys. Rev. Acc. and Beams 19, 024401 (2016)

[6] A. Blednykh, G. Bassi, Y. Hidaka, V. Smaluk, G. Stupakov, Low-frequency quadrupole impedance of undulators and wigglers, Phys. Rev. ST Accel. Beams 19, 104401 (2016).

[7] A. Chao, S. Heifets, and B. Zotter, Tune shifts of bunch trains due to resistive vacuum chambers without circular symmetry, Phys. Rev. ST Accel. Beams 5, 111001 (2002).

[8] J. Laslett, in Proceedings of the Summer Study on Storage Rings, Brookhaven, 1963 (BNL, Brookhaven, NY, 1963), pp. 324?367.